J. Biophotonics **5**, No. 2, 140–151 (2012) / **DOI** 10.1002/jbio.201100082

Journal of BIOPHOTONICS

FULL ARTICLE

Microvascular and mitochondrial PO_2 simultaneously measured by oxygen-dependent delayed luminescence

Sander I. A. Bodmer[1], *Gianmarco M. Balestra*[2], *Floor A. Harms*[1], *Tanja Johannes*[1], *Nicolaas J. H. Raat*[1], *Robert J. Stolker*[1], *and Egbert G. Mik*[*,1,3]

[1] Department of Anesthesiology, Laboratory of Experimental Anesthesiology, Erasmus MC – University Medical Center Rotterdam, s-Gravendijkwal 230, 3015 CE, Rotterdam, The Netherlands
[2] Department of Intensive Care, University Hospital Basel, Basel, Switzerland
[3] Department of Intensive Care, Erasmus MC – University Medical Center Rotterdam, Rotterdam, The Netherlands

Received 7 September 2011, revised 3 November 2011, accepted 3 November 2011
Published online 25 November 2011

Key words: oxygen-dependent quenching, phosphorescence, delayed fluorescence, lifetime measurement, oxygen measurement, tissue oxygen, protoporphyrin IX, Oxyphor G2, Pd-porphyrin

Measurement of tissue oxygenation is a complex task and various techniques have led to a wide range of tissue PO_2 values and contradictory results. Tissue is compartmentalized in microcirculation, interstitium and intracellular space and current techniques are biased towards a certain compartment. Simultaneous oxygen measurements in various compartments might be of great benefit for our understanding of determinants of tissue oxygenation. Here we report simultaneous measurement of microvascular PO_2 (μPO_2) and mitochondrial PO_2 ($mitoPO_2$) in rats. The μPO_2 measurements are based on oxygen-dependent quenching of phosphorescence of the near-infrared phosphor Oxyphor G2. The $mitoPO_2$ measurements are based on oxygen-dependent quenching of delayed fluorescence of protoporphyrin IX (PpIX). Favorable spectral properties of these porphyrins allow simultaneous measurement of the delayed luminescence lifetimes. A dedicated fiber-based time-domain setup consisting of a tunable pulsed laser, 2 red-sensitive gated photomultiplier tubes and a simultaneous sampling data-acquisition system is described in detail. The absence of cross talk between the channels is shown and the feasibility of simultaneous μPO_2 and $mitoPO_2$ measurements is demonstrated in rat liver in vivo. It is anticipated that this novel approach will greatly contribute to our understanding of tissue oxygenation in physiological and pathological circumstances.

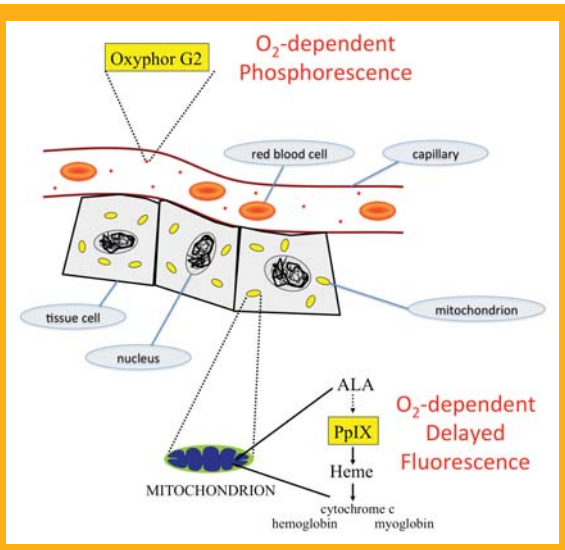

Schematic representation of the measuring concept.

* Corresponding author: e-mail: e.mik@erasmusmc.nl, Phone: +31 10 7043310, Fax: +31 10 7044725

1. Introduction

The study into the determinants of tissue oxygenation in physiological and pathological circumstances is a complex field of ongoing research. Tissue oxygen tension (tPO_2) is a key parameter for physiological function. Because of its importance many techniques have been developed to measure tPO_2 in vivo [1]. Concerning oxygenation, tissue can be regarded to consist of three main compartments, the microcirculation, the interstitial space and the intracellular space. Due to the technological and physical-chemical background of the available techniques to measure tPO_2, each is biased towards a certain compartment. Oxygen electrodes [2] tend to measure interstitial PO_2 while e.g. phosphorescence quenching [3] and electron paramagnetic resonance oximetry [4] are biased towards the microcirculation. Since oxygen gradients exist between the compartments this results in a bias towards a specific PO_2 range. This bias, together with technical differences like response time and sample volume, have made the interpretation and comparison of in vivo oxygen measurements difficult [5]. Therefore, the simultaneous measurement of PO_2 in different tissue compartments is needed to further our understanding of oxygen delivery and utilization under various pathophysiological circumstances.

Oxygen-dependent quenching of phosphorescence is a powerful method for quantitative measurement of PO_2 in biological samples [6]. Pd-meso-tetra-(4-carboxyphenyl)-tetrabenzoporphyrin (Oxyphor G2) is a relatively new phosphor which is excellently suited for oxygen measurements in vivo [7–9]. It is highly soluble in blood plasma, where it binds to albumin and confines to the circulation [10]. Upon intravascular injection oxygen-dependent phosphorescence lifetimes can be measured at the surface of tissues and organs using e.g. fiber-based phosphorimeters [11, 12]. In this way, Oxyphor G2 has been successfully used for measurement of the distribution of microvascular oxygen pressure (μPO_2) in e.g. solid tumors [13] and kidney [14, 15]. Oxyphor G2 has its absorption maxima at 440 and 632 nm and its emission near 800 nm.

Recently we reported that the delayed fluorescence lifetime of endogenous PpIX can be used to measure mitochondrial PO_2 ($mitoPO_2$) in cultured cells [16] and in vivo [17–19]. Administration of the precursor 5-aminolevulinic acid (ALA) increases the intramitochondrial levels of PpIX, and $mitoPO_2$ can subsequently be measured by its oxygen-dependent delayed fluorescence lifetime. Delayed fluorescence has much in common with phosphorescence and it shares the useful possibility to determine heterogeneity in PO_2 within a volume of tissue with high temporal resolution [20, 21]. Moreover, the basic setup for delayed fluorescence lifetime measurements resembles the equipment for phosphorescence quenching experiments. Therefore, simultaneous measurement of phosphorescence and delayed fluorescence should be possible. The spectral properties of Oxyphor G2 and PpIX are very favorable in this respect with having a common excitation band (632 nm) and widely separated emission bands (~800 nm for Oxyphor G2 and ~690 nm for PpIX). The successful combination of the two techniques would provide a powerful means to measure simultaneously μPO_2 and $mitoPO_2$ in vivo.

Accordingly, we have developed a delayed luminescence lifetime technique that quantitatively and simultaneously measures μPO_2 using the oxygen-dependent optical properties of injectable Oxyphor G2 and $mitoPO_2$ using the oxygen-dependent optical properties of ALA-enhanced PpIX. In this paper we describe in detail the setup and the applicability of this technique for simultaneous measurements of μPO_2 and $mitoPO_2$ in intact tissue. The lack of cross-over in the detection channels is demonstrated in vivo in the rat. Ultimately we provide the first simultaneous measurements of μPO_2 and $mitoPO_2$ in the rat liver in vivo.

2. Materials and methods

2.1 The measurement concept

Both Oxyphor G2 and PpIX possess a first excited triplet state (T_1) that reacts strongly with oxygen. Population of T_1 occurs upon photo excitation with light at one of the porphyrin-specific absorption bands. Energy transfer between the excited porphyrin and oxygen results in an oxygen-dependent T_1 lifetime. Spontaneous relaxation of the T_1 state to the ground state (S_1) produces delayed luminescence (i.e. phosphorescence or delayed fluorescence) that can be used to measure the T_1 lifetime (Figure 1). The lifetime of the delayed luminescence is quantitatively related to the oxygen tension by the Stern-Volmer relationship:

$$PO_2 = \frac{\frac{1}{\tau} - \frac{1}{\tau_0}}{k_q} \quad (1)$$

where PO_2 is the oxygen tension (in mm Hg), τ is the measured decay time, k_q is the quenching constant (in mm Hg^{-1} s^{-1}) and τ_0 is the lifetime at an oxygen pressure of zero.

Oxyphor G2 is a water-soluble synthetic porphyrin especially developed as oxygen-sensitive phosphorescent dye. Absorption maxima of Oxyphor G2 are 440 and 632 nm and emission peaks around 800 nm. The calibration constants of Oxyphor G2

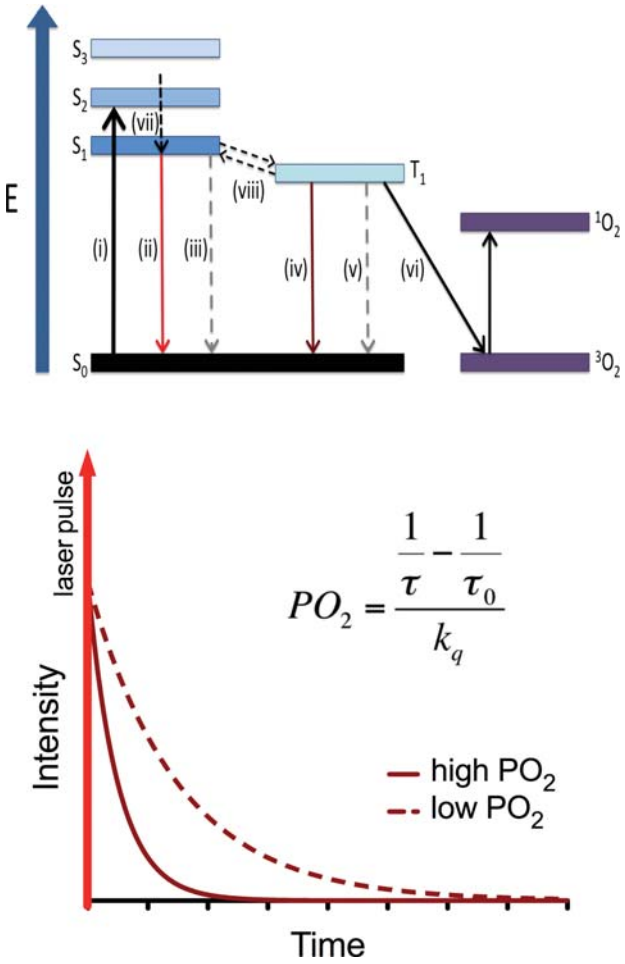

Figure 1 (online color at: www.biophotonics-journal.org) Jablonski diagram of states and state transitions of PpIX and its interaction with oxygen (upper panel) and the principle of measuring oxygen tension (PO_2) by oxygen dependent quenching of delayed luminescence (lower panel). S_0, S_1, S_2 and S_3 represent the ground state and first, second and third excited singlet states, respectively. T_1 represent the first excited triplet states of PpIX and $^3O_2$ and $^1O_2$ are the triplet ground state and excited singlet state of oxygen. Absorption (i), fluorescence and delayed fluorescence (ii), radiationless transitions (iii and v), phosphorescence (iv), energy transfer (vi), internal conversion (vii) and bi-directional intersystem crossing (viii). The inserted equation in the lower panel is the Stern-Volmer relationship in which PO_2 is the oxygen tension, τ is the measured lifetime, k_q is the quenching constant and τ_0 is the lifetime in the absence of oxygen.

for in vivo conditions are $k_q = 270$ mm Hg^{-1} s^{-1} and $\tau_0 = 250$ µs and the quantum efficiency of phosphorescence is approximately 12% [9]. The oxygen-dependent quenching of phosphorescence of Oxyphor G2 has been successfully used for microvascular (μPO_2) measurements [11, 13–15] and PO_2 measurements in macrovessels [22]. To this end, Oxyphor G2 is injected into the blood stream of experimental animals where the probe binds to albumin and is confined to the circulation [10]. Typical in vivo concentrations of Oxyphor G2 for microvascular oxygen measurements are around 1 nmol/g (tissue wet weight).

Protoporphyrin IX (PpIX) is the final precursor of heme in the heme biosynthetic pathway. PpIX is synthesized in the mitochondria [23] and administration of its precursor 5-aminolevulinic acid (ALA) to cells and organisms substantially enhances PpIX concentration [24]. Since the conversion of PpIX to heme is a rate-limiting step, administration of ALA causes accumulation of PpIX in the mitochondria [19]. Besides the absorption maximum around 420 nm the absorption spectrum of PpIX contains several smaller peaks including one around 634 nm (Figure 2). The fluorescence spectrum is typically two-peaked. Because of the spectral overlap with the excitation pulse only the peak around 690 nm is used for delayed fluorescence detection. The oxy-

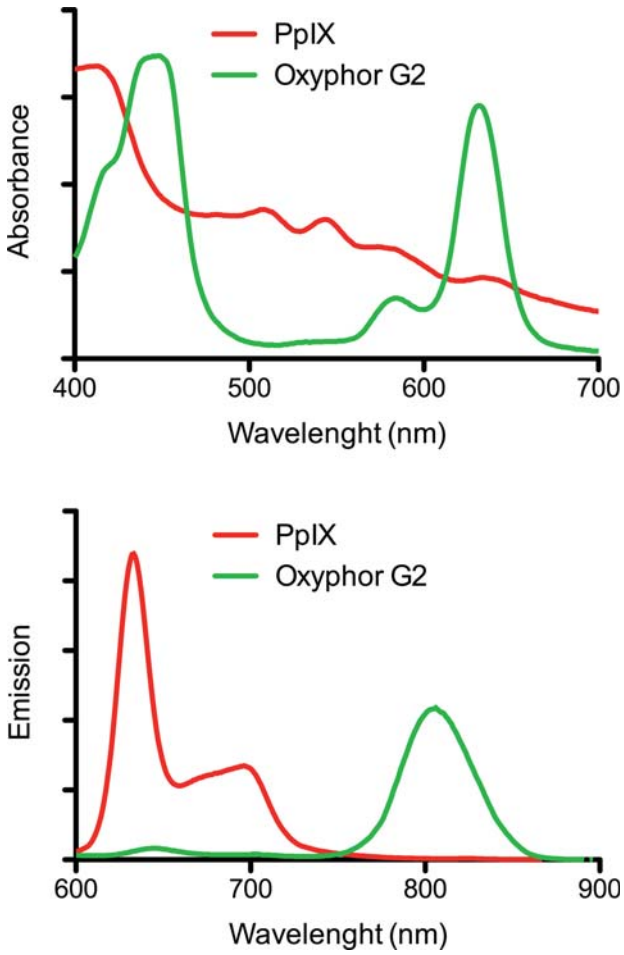

Figure 2 (online color at: www.biophotonics-journal.org) Absorption spectra (upper panel) and emission spectra (lower panel) of Oxyphor G2 and PpIX.

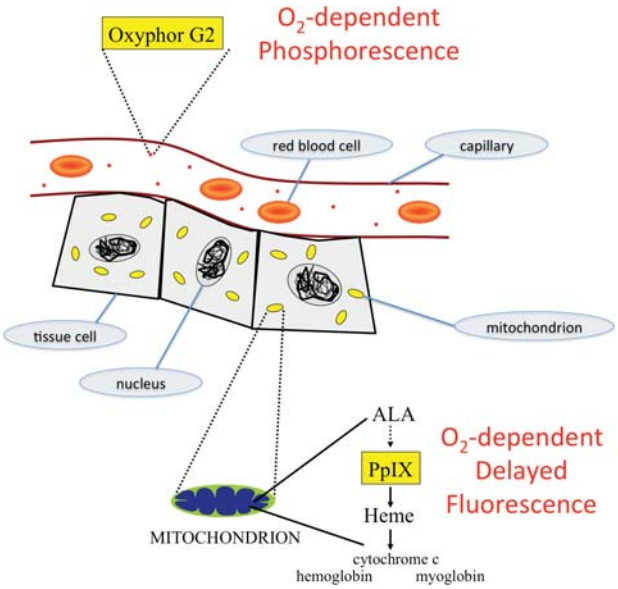

Figure 3 (online color at: www.biophotonics-journal.org) Schematic representation of the measuring concept. Oxyphor G2 is directly injected into the bloodstream and is used as microvascular oxygen probe by means of oxygen-dependent quenching of phosphorescence. PpIX is induced in the mitochondria by administration of its precursor ALA and is used as mitochondrial oxygen probe by means of oxygen-dependent quenching of delayed fluorescence.

gen-dependent delayed fluorescence of PpIX has been successfully introduced as a technique for mitochondrial oxygen measurements [16, 18, 19]. The calibration constants of PpIX for in vivo conditions are $k_q = 830\ \text{mm Hg}^{-1}\,\text{s}^{-1}$ and $\tau_0 = 0.8$ ms. ALA-induced PpIX levels have been reported to be in the order of 20 nmol/g (tissue wet weight) in liver [25].

Both Oxyphor G2 and PpIX can be effectively excited with red light at a wavelength around 632 nm. This allows simultaneous excitation within a single measurement volume. The emission peaks are well separated without spectral overlap. Therefore, in principle, these spectral properties make the two porphyrins excellently suited for simultaneous excitation and separate detection. The intravascular localization of Oxyphor G2 combined with the mitochondrial localization of PpIX therefore enables simultaneous measurement of μPO_2 and $\text{mito}PO_2$ (Figure 3).

2.2 *Delayed luminescence setup*

A schematic drawing of the experimental setup is shown in Figure 4. A compact computer-controlled tunable laser (Opolette 355-I, Opotek, Carlsbad, CA, USA), providing pulses with a specified duration of 4–10 ns and typically 2–4 mJ/pulse over the tunable range of 410 to 670 nm, was used as excitation source. The laser was coupled into a Fiber Delivery System (Opotek, Carlsbad, CA, USA) consisting of 50 mm planoconvex lens, X–Y fibermount and a 2 meter fiber with a core diameter of 1000 µm. This fiber was coupled to the excitation branch of a bifurcated reflection probe (FCR-7IR400-2-ME, Avantes b.v., Eerbeek, The Netherlands) by an In-Line Fiber Optic Attenuator (FOA-Inline, Avantes b.v., Eerbeek, The Netherlands). The light output of the excitation branch was set at 200 µJ/pulse as measured by a FieldMate laser power meter with PowerMax PS19 measuring head (Coherent Inc., Santa Clara, CA, USA). The emission branch of the

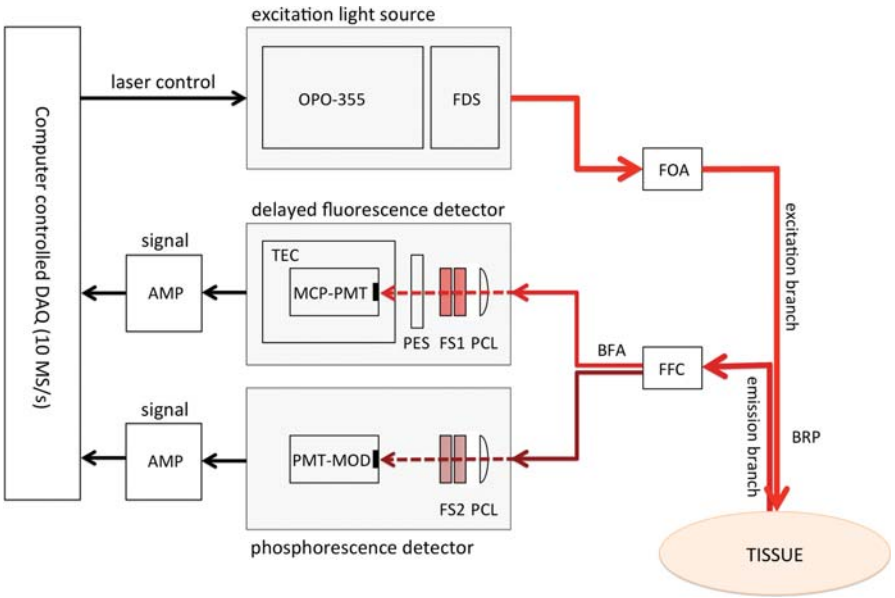

Figure 4 (online color at: www.biophotonics-journal.org) Schematic drawing of the experimental setup. OPO-355: Opolette 355-I, FDS: Fiber Delivery System, FOA: Fiber Optic Attenuator, BFP: Bifurcated Reflection Probe, FFC: Fiber to Fiber Coupling, BFA: Bifurcated Fiber Assembly, PCL: Plano Convex Lens, FS1 & FS2: Filter Sets, PES: Protective Electronic Shutter, MCP-PMT: Micro Channel Plate Photomultiplier Tube, TEC: Thermo Electric Cooling, PMT-MOD: Photomultiplier Module, AMP: Amplifier, DAQ: Data Acquisition.

reflection probe was coupled to a bifurcated fiber assembly (Model 77533, Newport, Irvine, CA, USA), which acted as splitter for the two detection channels.

The PpIX signal was detected by a gated microchannel plate photomultiplier tube (MCP-PMT R5916U series, Hamamatsu Photonics, Hamamatsu, Japan). The MCP-PMT was custom adapted with an enhanced red-sensitive photocathode having a quantum efficiency of 24% at 650 nm. The MCP-PMT was mounted on a gated socket assembly (E3059-501, Hamamatsu Photonics, Hamamatsu, Japan) and cooled to −30 °C by a thermoelectric cooler (C10373, Hamamatsu Photonics, Hamamatsu, Japan). The MCP-PMT was operated at a voltage in the range of 2300–3000V by a regulated high-voltage DC power supply (C4848-02, Hamamatsu Photonics, Hamamatsu, Japan). One branch of the bifurcated fiber (splitter) was fit into an Oriel Fiber Bundle Focusing Assembly (Model 77799, Newport, Irvine, CA, USA) which was coupled to the MCP-PMT by an in-house built optics consisting of a filter-holder, a plano convex lens (BK-7, OptoSigma, Santa Ana, CA, USA) with focal length of 90 mm and an electronic shutter (04 UTS 203, Melles Griot, Albuquerque, NM, USA). The shutter was controlled by an OEM Shutter Controller Board (59 OSC 205, Melles Griot, Albuquerque, NM, USA) and served as protection for the PMT, which was configured for the "normally on" mode. The PpIX emission light was filtered by a combination of a 590 nm longpass filter (OG590, Newport, Irvine, CA, USA) and a broadband (675 ± 25 nm) bandpassfilter (Omega Optical, Brattleboro, VT, USA).

The Oxyphor G2 signal was detected by a photomultiplier module with gate function (H10304-20-NN, Hamamatsu Photonics, Hamamatsu, Japan). The second branch of the bifurcated fiber (splitter) was fit into an Oriel Fiber Bundle Focusing Assembly (Model 77799, Newport, Irvine, CA, USA) which was coupled to the PMT-module by an in-house built optics consisting of a filter-holder, a plano convex lens (BK-7, OptoSigma, Santa Ana, CA, USA) with focal length of 90 mm. The Oxyphor G2 emission light was filtered by a combination of a 715 nm longpass filter (RG715, Newport, Irvine, CA, USA) and a 790 ± 20 nm bandpassfilter (Omega Optical, Brattleboro, VT, USA).

The output currents of the photomultipliers were voltage-converted by in-house built amplifiers with an input impedance of 440 ohm, 400 times voltage amplification and a bandwidth around 20 Mhz. Data-acquisition was performed by a PC-based data-acquisition system containing a 10 MS/s simultaneous sampling data-acquisition board (NI-PCI-6115, National Instruments, Austin, TX). The amplifiers were coupled to the DAQ-board by a BNC interface (BNC-2090A, National Instruments, Austin, TX). The data-acquisition ran at a rate of 10 mega samples per second and 64 laser pulses (repetition rate 20 Hz) were averaged prior to analysis. Control of the setup and analysis of the data was performed with software written in LabView (Version 8.6, National Instruments, Austin, TX, USA).

2.3 Analysis of delayed luminescence

In case of non-homogeneous oxygen tension the delayed luminescence signal can in general be described by an integral over an exponential kernel:

$$y(t) = \int_0^t \exp(-\lambda t)\, f(\lambda)\, \mathrm{d}\lambda \tag{2}$$

where $f(\lambda)$ denotes the spectrum of reciprocal lifetimes within the finite data set $y(t)$. Mono-Exponential Analysis (MEA) in generally overestimates the average lifetime and consequently underestimates the PO_2 within the sample volume [11]. A much better estimate of the average PO_2 and an indication of its heterogeneity can be obtained by the approach described by Golub et al. [20]. They demonstrated that the heterogeneity in oxygen pressure could be analyzed by fitting distributions of quencher concentration to the delayed luminescence data. Corresponding to their work, the fitting function for a simple rectangular distribution with a mean PO_2 Q_m and a PO_2 range from $Q_m - \delta$ till $Q_m + \delta$ is:

$$Y_R = \exp(-(k_0 + k_q Q_m)\, t) \cdot \frac{\sin \mathrm{h}\,(k_q\, \delta t)}{k_q\, \delta t} \tag{3}$$

where $Y(t)$ is the normalized delayed fluorescence data, k_0 is the first-order rate constant for delayed fluorescence decay in the absence of oxygen, k_q is the quenching constant and δ is half the width of the rectangular distribution. In terms of quenching constants and the Stern-Volmer relationship, Eq. (3) can be rewritten as:

$$Y_R = \exp\left(-\left(\frac{1}{\tau_0} + k_q \langle \mathrm{PO_2} \rangle\right) t\right) \cdot \frac{\sin \mathrm{h}\,(k_q\, \delta t)}{k_q\, \delta t} \tag{4}$$

where $\langle PO_2 \rangle$ is the mean PO_2 within the sample volume and τ_0 the lifetime in the absence of oxygen. The standard deviation (σ) can be retrieved from δ by:

$$\sigma = \frac{\delta}{\sqrt{3}} \tag{5}$$

This approach was successfully used by our group in phosphorescence lifetime measurements [11]. Recently we demonstrated that the approach is also useful for delayed fluorescence lifetime measurements in the case of complex underlying lifetime distributions [17]. Analysis of the delayed luminescence signals by means of equations 3–4 is referred to as the Rectangular Distribution Method (RDM).

Analysis of the photometric signals, by means of MEA and RDM, was performed with software written in LabView (Version 8.6, National Instruments, Austin, TX, USA), using the Marquart-Levenberg non-linear fit procedure.

2.4 Analysis of influence of noise

Signal-to-noise ratio (SNR) in time domain lifetime measurements is commonly defined as the ratio of maximal signal amplitude (at the start of the decay) to the maximum signal of the noise (peak-to-peak). The negative effects of noise on the accuracy of the measurement are inversely related to the lifetime. Therefore, the presence of noise especially degrades measurement accuracy at higher PO_2 levels.

Because the quenching constants of PpIX and Oxyphor G2 are not the same, the effect of noise on the accuracy of μPO_2 and $mitoPO_2$ measurements differs. We analyzed the relationship between measurement accuracy, PO_2 and SNR of the two channels by means of computer simulations. In steps of 10 mm Hg, over a PO_2 range of 0–300 mm Hg, we simulated delayed fluorescence and phosphorescence traces. SNR was varied by adding different amounts of Poisson distributed noise to the simulated decays (SNR 5, 10, 20 and 50). The PO_2 was calculated back from the noisy signal by lifetime analysis. The noise-induced error was calculated as the absolute difference between simulated PO_2 and recovered PO_2. We performed 500 simulation runs per PO_2 step and defined the potential noise-induced error as the maximum error occurring during these 500 runs.

2.5 Measurement of spectral properties

Absorption spectra were recorded using a Hitachi U-3000 Spectrophotometer (Hitachi High-Technologies Corporation, Tokyo, Japan). Emission spectra were recorded using a Hitachi F-4500 Fluorescence Spectrophotometer (Hitachi High-Technologies Corporation, Tokyo, Japan). Both Oxyphor G2 and PpIX were dissolved in phosphate buffered saline containing 4% bovine serum albumin (Sigma-Aldrich, St. Louis, MO, USA) to a final concentration of 10 μM. Emission spectra were recorded after deoxygenating the sample by flushing with nitrogen.

2.6 Animal preparation

The experimental protocol was approved by the Animal Research Committee of the ErasmusMC – University Medical Center Rotterdam. Animal care and handling were performed in accordance with the guidelines for Institutional and Animal Care and Use Committees (IACUC) and done by trained staff of the Erasmus Experimental Animal Facility.

A total of 15 male Wistar rats (Charles River, Wilmington, MA) with a bodyweight of 275–325 gram were used. Rats received either a combination of 200 mg/kg 5-aminolevulinic acid (ALA, Sigma-Aldrich, St. Louis, MO, USA) and 0.4 mg/kg Oxyphor G2 (Oxygen Enterprises, Philadelphia, PA, USA) ($n = 10$) or only Oxyphor G2 ($n = 5$). In order to ensure an optimal mitochondrial PpIX concentration, ALA was administered by intraperitoneal injection 2.5 hours before start of experimental procedures. Animals were anesthetized by an intraperitoneal injection of a mixture of Ketamine (90 mg/kg, Alfasan, Woerden, The Netherlands), Medetomidine (0.5 mg/kg, Sedator Eurovet Animal Health BV, Bladel, The Netherlands) and Atropine (0.05 mg/kg, Centrofarm Services BV, Etten-Leur, The Netherlands). A continuous intravenous infusion of Ketamine (50 mg/kg/hr) was used for maintaining anesthesia. A tracheotomy was performed prior to starting mechanical ventilation. Mechanical ventilation, using a Babylog 8000 ventilator (Dräger, Dräger Medical Netherlands BV, Zoetermeer, The Netherlands), was controlled and adjusted on end-tidal PCO_2 (~35 mm Hg).

A catheter (sterilized 0.9 mm diameter polyethylene catheter) was inserted in the right jugular vein for intravenous administration of anesthetics, Oxyphor G2 and fluids (0.9% NaCl, 5 mL kg^{-1} h^{-1}). A similar catheter was placed in the right carotid artery to monitor arterial blood pressure (MAP) using a Powerlab 8/30 data-acquisition system with LabChart Pro (ADInstruments, Bella Vista NSW, Australia). This catheter was also used for taking arterial blood gases. The animal was placed onto a heating pad and body temperature was rectally measured and kept around 37 °C.

A midline laparotomy was performed to gain access to the liver for measuring μPO_2 and $mitoPO_2$. Before infusion of Oxyphor G2, 20 minutes prior to the start of the actual oxygen measurements, signals were recorded for examination of cross talk between the channels. This was repeated after administration of Oxyphor G2. Measurements were performed in dimmed light, after assuring proper positioning of the reflection probe. ALA was dissolved in phosphate buffered saline (PBS) and adjusted to pH 7.4 prior to injection. Oxyphor G2 was dissolved in PBS (1.25 mg/ml) as stock solution.

Variations in inspired oxygen fraction (FiO_2) were made during the protocol at set time points by mixtures of oxygen and nitrogen. Instrumentation and Oxyphor G2 administration were performed while breathing 40% oxygen (0.4 FiO_2). After first measurements at 0.4 FiO_2, FiO_2 was set to 1.0 and

after a stabilization period of 20 min the second measurements were performed. Then FiO_2 was set to 0.2 and again after a stabilization period of 20 min the third measurements were performed. In the time control group ($n = 5$) FiO_2 was set at 0.4 during the entire experiment. At the end of the experimental protocol animals were euthanized by an overdose of Euthasol (ST Farma, Raamsdonksveer, The Netherlands).

2.7 *Statistical analysis*

Data are expressed as mean ± standard deviation (s.d.) unless stated otherwise. Repeated-measures analysis of variance, one-way ANOVA with Bonferroni posttest, was used to analyze the effect of changes in FiO_2 on physiological parameters. Two-way ANOVA for repeated measurements with Bonferroni posttest was used to analyze differences between μPO_2 and $mitoPO_2$ at the various FiO_2 settings. $P < 0.05$ was considered significant.

3. Results

In order to measure signals of different porphyrins simultaneously, it is mandatory that the readings do not mutually interfere. The wide spectral separation of the emissions of PpIX and Oxyphor G2, 690 nm and 790 nm respectively, indicate this should be possible to achieve. Indeed, as is shown in Figure 5, there was no interference of the two signals. Injec-

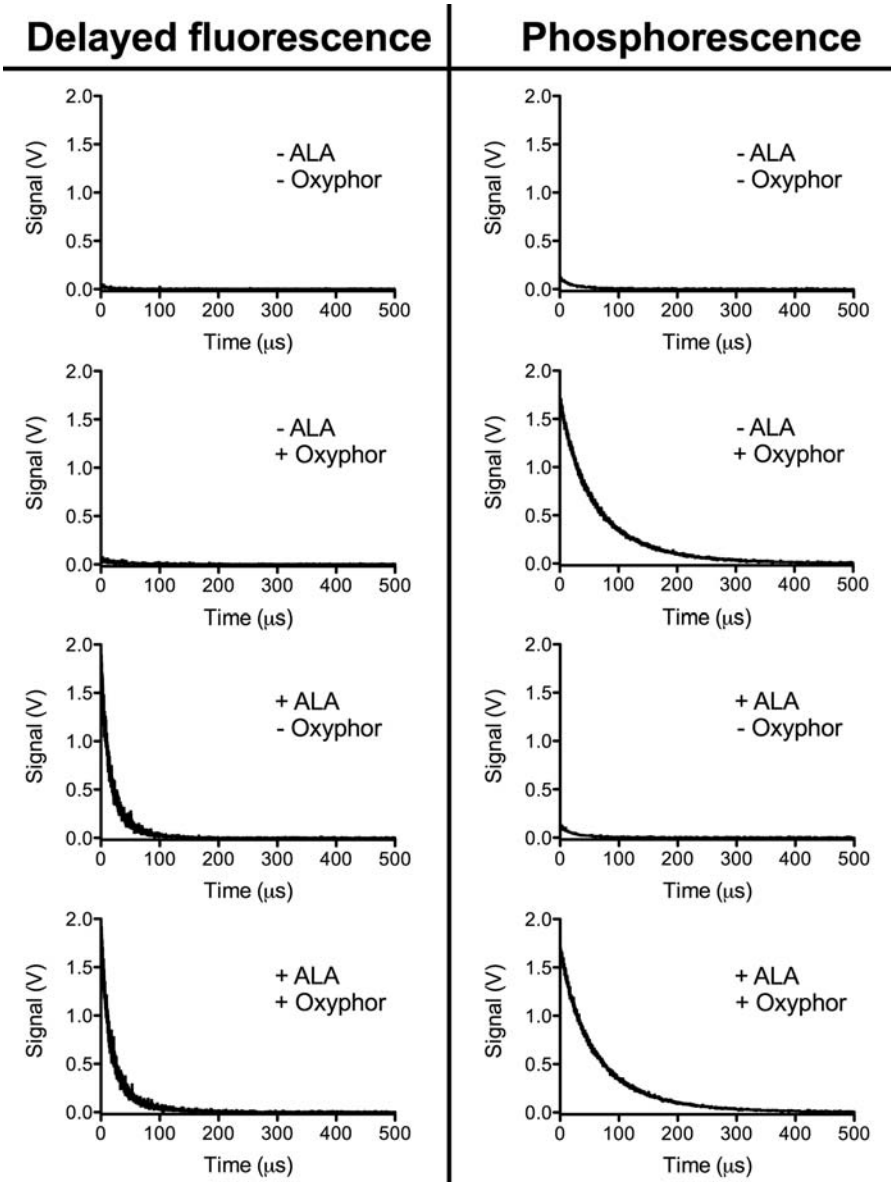

Figure 5 Signals obtained from both channels with and without various combinations of probes. Delayed fluorescence at 690 nm and phosphorescence at 790 nm simultaneously measured after excitation at 632 nm. ALA: 200 mg/kg 5-aminolevulinic acid, Oxyphor: 0.4 mg/kg Oxyphor G2.

tion of ALA induced a clear delayed fluorescence signal in the 690 nm channel, indicating buildup of mitochondrial PpIX within the liver. In contrast, ALA administration did not induce any signal in the 790 nm channel. While injection of Oxyphor G2 induced a readily measurable phosphorescence signal at 790 nm, it was not detectable in the 690 nm channel. In both channels a faint decaying signal was observed in the absence of porphyrins. This background was not oxygen-sensitive and most probably originated from the glass in the fiber optic. Overall this background accounted to less than 5% of the total signal and no background corrections were made in the signal analysis.

Noise is inevitably present in real signals and generally has a negative effect on the accuracy of measurements. Because the quenching constants for μPO_2 and $mitoPO_2$ differ, the dynamic range of measure lifetimes differs between the channels. Interpretation of simultaneous measurements could be hampered by inter channel differences in noise sensitivity. Therefore we analyzed the relationship between accuracy, PO_2 and SNR by means of computer simulations (Figure 6). It is evident that both channels behave differently, with the delayed fluorescence measurement being more sensitive to the deleterious effects of noise. However, in practice, SNR $>$ 20 is readily achieved for both PpIX and Oxyphor G2. In that case, the noise-induced potential error in both channels is below 2% over a large PO_2 range.

In general, the oxygen tension in tissue is non-homogeneous because of the existence of oxygen gradients as a result of oxygen consumption and diffusion. Delayed luminescence of oxygen-sensitive probes is therefore not decaying mono-exponentially but the photometric signals contain lifetime distributions. Figure 7 shows an example of a phosphores-

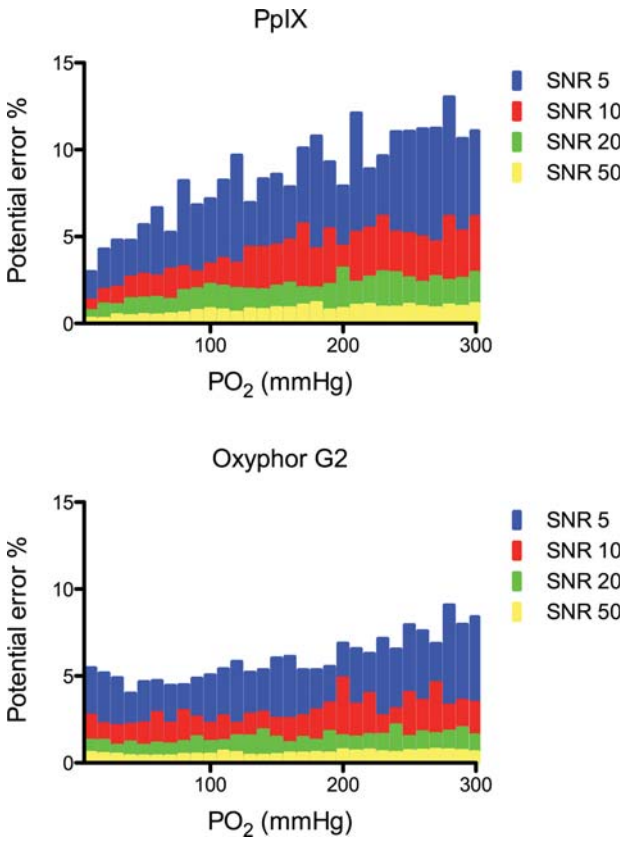

Figure 6 (online color at: www.biophotonics-journal.org) Noise-induced potential error in PO_2 retrieval as result of the presence of noise in delayed fluorescence (upper panel) and phosphorescence (lower panel) signals. SNR: signal-to-noise ratio.

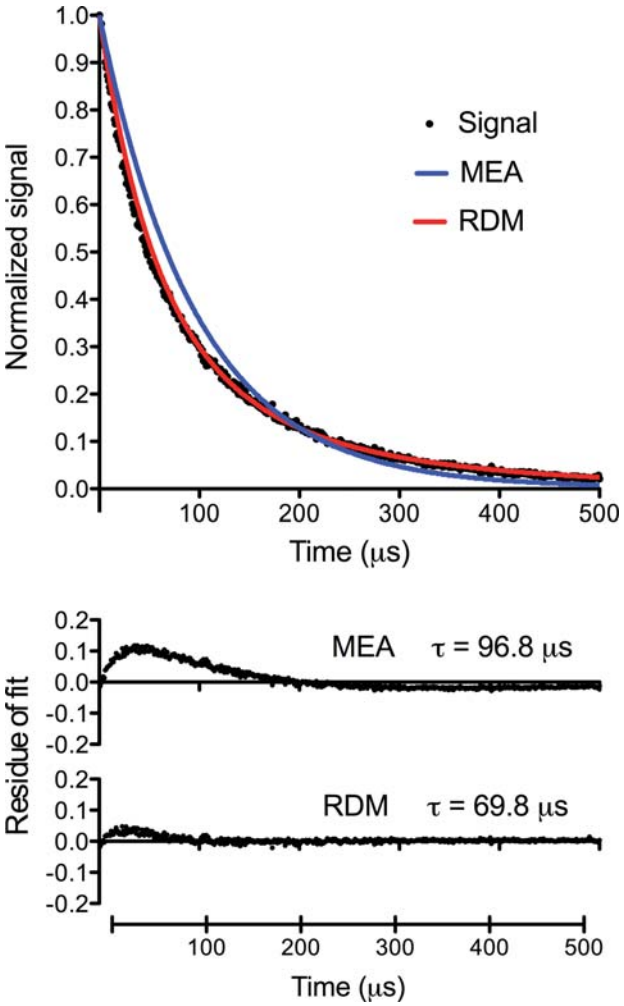

Figure 7 (online color at: www.biophotonics-journal.org) Example of two different fit procedures on a phosphorescence signal measured in in vivo rat liver at 0.4 FiO_2. Raw phosphorescence decay data and the corresponding curves of two fit procedures (upper panel). Residue of fit (difference between data and fit) for both fit procedures and the obtained phosphorescence lifetimes. MEA, mono-exponential analysis; RDM, rectangular distribution method.

cence trace from Oxyphor G2 measured in rat liver at 0.4 FiO_2 (= 40% oxygen). Mono-exponential analysis (MEA) resulted in a poor fit and, compared to the rectangular distribution method (RDM), resulted in a relatively long phosphorescence lifetime. In the case of MEA the lifetime was 96.8 μs, corresponding to a μPO_2 of 23.4 mm Hg. The RDM resulted in a lifetime of 69.8 μs, corresponding to an average μPO_2 of 38.2 mm Hg. The remaining small difference between data and RDM curve fit at early times reflects the fact that a rectangular distribution is only an estimation of the real oxygen distribution.

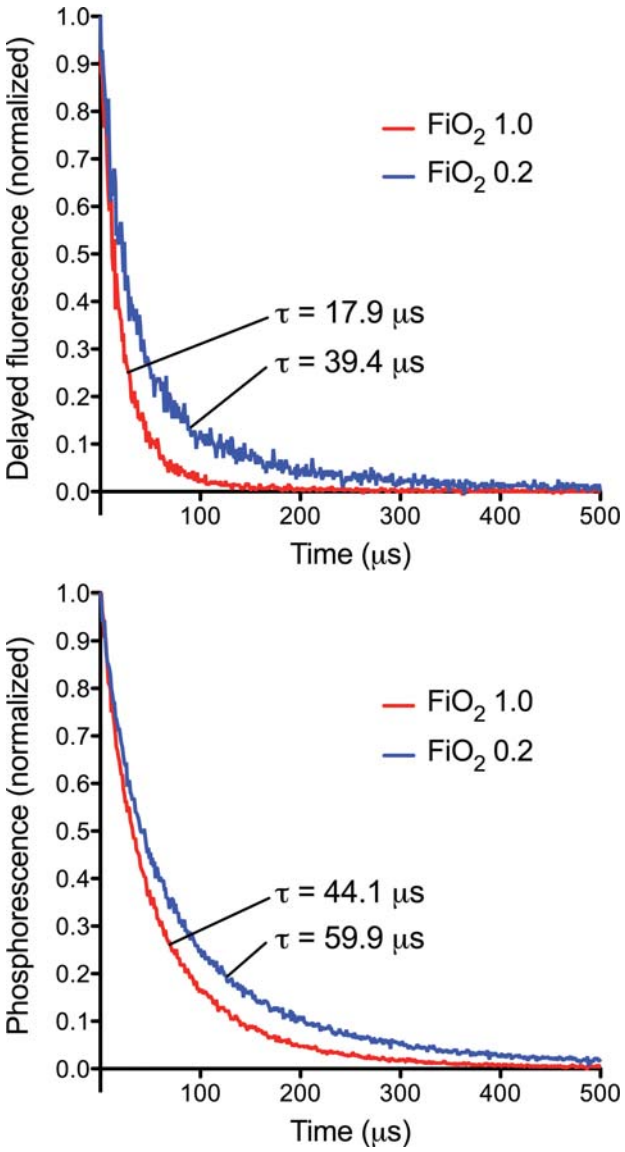

Figure 8 (online color at: www.biophotonics-journal.org) Examples of delayed luminescence data measured at two different inspired oxygen fractions (FiO_2). Delayed fluorescence from PpIX (upper panel) and phosphorescence from Oxyphor G2 (lower panel). Lifetimes were obtained by RDM analysis.

An example of a simultaneous measurement of PpIX delayed fluorescence and Oxyphor G2 phosphorescence is shown in Figure 8. Both signals showed clear oxygen-sensitivity, with the lifetime becoming visually longer at a lower inspired oxygen fraction. The lifetimes of PpIX delayed fluorescence were 17.9 μs at 1.0 FiO_2 and 39.4 μs at 0.2 FiO_2, corresponding to an average $mitoPO_2$ of 65.8 mm Hg and 29.1 mm Hg respectively. The lifetimes of Oxyphor G2 phosphorescence were 44.1 μs at 1.0 FiO_2 and 59.9 μs at 0.2 FiO_2, corresponding to an average μPO_2 of 69.2 mm Hg and 47.0 mm Hg respectively.

Simultaneous measurements of liver $mitoPO_2$ and μPO_2 at three FiO_2 steps were performed in a series of 5 rats. An overview of physiological variables is given in Table 1. Arterial PO_2, as measured by bloodgas analysis, significantly differed between the FiO_2 steps, being approximately 5 times higher at 1.0 FiO_2 compared to 0.2 FiO_2. From the other variables only the MAP at 0.2 FiO_2 is significantly lower than MAP at 0.4 and 1.0 FiO_2. End-tidal CO_2 and temperature were actively controlled by ventilation and external heating. Heart rate and hemoglobin concentration were stable during the FiO_2 steps.

Figure 9 shows the results of the simultaneous measurements of $mitoPO_2$ and μPO_2 at various FiO_2 settings. Both $mitoPO_2$ and μPO_2 increased at higher FiO_2, and there were significant differences between 0.2 FiO_2 and 1.0 FiO_2 and between 0.4 FiO_2 and 1.0 FiO_2. Furthermore, at all FiO_2 settings the average $mitoPO_2$ was a little lower than the average μPO_2 but only at 1.0 FiO_2 this difference was statistically significant. The standard deviation, as a measure of heterogeneity obtained from the RDM, was significantly higher for μPO_2 compared to $mitoPO_2$ at all FiO_2 settings. At 1.0 FiO_2 the heterogeneity in μPO_2 was significantly higher compared to the heterogeneity in μPO_2 at 0.2 FiO_2. In the time control group at 0.4 FiO_2 μPO_2 and $mitoPO_2$ and their heterogeneity were stable over time and similar to the experimental group at 0.4 FiO_2.

Table 1 Physiological values measured during in vivo experiments at FiO_2 of 0.2, 0.4 and 1.0. A significant difference (*) was noted in the arterial PO_2 between the FiO_2 steps and in the MAP between FiO_2 of 0.2 and the other steps. No significant difference was measured between conditions for the remaining physiological variables.

Physiological variables	$FiO_2 = 0.2$	$FiO_2 = 0.4$	$FiO_2 = 1.0$
PO_2 (mm Hg)*	93 ± 12	191 ± 15	481 ± 35
$EtCO_2$ (mm Hg)	36 ± 2	34 ± 4	33 ± 3
Hb (mmol/L)	8.0 ± 0.4	8.2 ± 0.7	8.1 ± 0.9
MAP (mm Hg)*	87 ± 15	109 ± 10	105 ± 10
Temp (°C)	37.1 ± 0.6	36.9 ± 0.5	37.0 ± 0.7
HR (beats/min)	248 ± 9	256 ± 18	251 ± 16

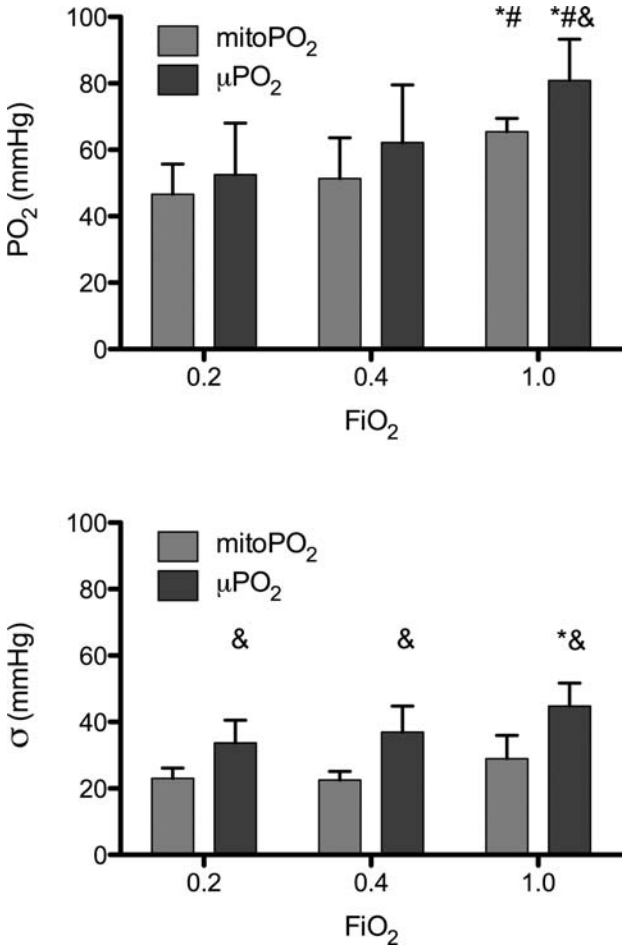

Figure 9 Microvascular and mitochondrial PO_2 in rat liver at different FiO_2 values. Average PO_2 as obtained by RDM analysis (upper panel) and corresponding standard deviation (lower panel). Significantly different compared to (*) 0.2 FiO_2, (#) 0.4 FiO_2 and (&) mitoPO_2.

4. Discussion and conclusion

In this work, we present a method to simultaneously measure oxygen tension in the mitochondria and microcirculation within intact living tissue. The method is based on a combination of oxygen-dependent quenching of delayed fluorescence of ALA-enhanced mitochondrial PpIX and oxygen-dependent quenching of phosphorescence of the exogenous dye Oxyphor G2. We comprehensively describe a time-domain based measurement system consisting of a tunable pulsed laser and two gated red-sensitive photomultipliers. The measurement equipment is fiber-based and can be easily used in (patho)physiological studies in small and large experimental animals. We demonstrate that the in vivo measured signals of PpIX and Oxyphor G2 do not interfere and that SNR $\geq$ 20 reduces noise-induced inaccuracy of both channels below 2%. Furthermore, we provide data of the first simultaneous measurements of mitoPO_2 and µPO_2, measured in rat liver in vivo during ventilation with various inspired oxygen fractions. To analyze the complex photometric signals we used RDM analysis, which provides the mean and standard deviation of the PO_2 in the measurement volume.

Our view on tissue oxygenation has gradually changed over years with the advent of novel technology to measure oxygen in tissues. Oxygen is supplied from blood to the tissues by passive diffusion and the site for oxygen exchange is the microcirculation. Although classically the capillary network was identified as the most likely site for oxygen to leave the bloodstream, a more modern view is that oxygen has the ability to diffuse from any microvessel along a large enough oxygen gradient [26]. Surrounding the microcirculation and in between the tissue cells is the interstitial space. Recent studies in resting skeletal muscle have indicated the existence of only a small gradient between microvessels and interstitium [27, 28]. The intracellular PO_2 and its influence on metabolism in vivo remains the most difficult to measure. Measurements of intracellular PO_2 have mostly been indirect, e.g. via measurement of myoglobin saturation [29]. Only recently it has become possible to measure directly PO_2 in mitochondria of living intact tissue [18, 19].

Since mitochondria are the oxygen consuming and energy producing organelles of cells, the development of a technique to measure mitoPO_2 removes the last hurdle in our ability to comprehensively measure tissue oxygenation. Especially in combination with microvascular PO_2 measurements it might be possible to gain direct insight in oxygen gradients and oxygen consumption. We previously used a combination of endogenously enhanced PpIX en Oxyphor G2 to measure, in cell suspensions, mitoPO_2 and extracellular PO_2 in culture medium [16]. These measurements were performed in cuvettes with separate devices that, unfortunately, could not be integrated into a useful in vivo measurement system. Therefore, we developed a dedicated fiber-based setup that allows simultaneous measurement of mitoPO_2 and µPO_2 in intact tissue using PpIX and Oxyphor G2.

In the current study we focused on the rat liver, since we have extensively evaluated the mitoPO_2 measurements in this type of tissue [19]. The measured mitoPO_2 values in the current study are very similar to our previously reported results. In light of the fact that intracellular PO_2 is generally expected to be low (several mm Hg) as a result of mitochondrial oxygen consumption, we were surprised to find such high mitoPO_2. However, mitoPO_2 values were well in the range of reported tissue PO_2 values measured by micro oxygen electrodes [30]. In our current study we can directly compare our mitoPO_2 measurements with the well-established phosphores-

cence lifetime technique. This direct comparison learns that only a small difference between mitoPO_2 and μPO_2 exists in liver. This latter is not surprising due to the anatomical structure of the liver, with very close proximity of tissue cells to blood and overall high blood supply. Furthermore, our findings fit well in the current view that tissue PO_2 might be much higher than classically reported with invasive techniques [31]. Indeed, a recent study using minimally invasive 19F MRI in a rat model found tissue PO_2 levels well above 50 mmHg in several organs including liver [32]. The standard deviation in μPO_2 obtained from the RDM analysis is larger than that for the mitoPO_2. This is most likely due to the size of the reflection probe. The measurement volume likely contains multiple microvessels that represent heterogenous PO_2.

Overall, our study shows that implementation of the technique to simultaneously measure μPO_2 and mitoPO_2 by oxygen-dependent delayed luminescence is feasible, based on a combination of exogenous Oxyphor G2 and endogenous PpIX. With ongoing evaluation of the use of the mitoPO_2 technique in other organs and tissues it is expected that this approach will greatly contribute to further our understanding of oxygen transport and oxygen metabolism in health and disease.

Acknowledgements This work was financially supported by the Young Investigator Grant 2009 (awarded to E.G.M.) from the Dutch Society of Anesthesiology. The authors thank Jacqueline Voorbeijtel and Patricia Specht for their expert biotechnical help. The authors thank dr. G. A. Koning and the Laboratory of Experimental Surgical Oncology of the ErasmusMC for help with the spectral measurements.

Conflict of Interest E.G.M is founder and shareholder of Photonics Healthcare B.V., a company aimed at making the delayed fluorescence lifetime technology available to a broad public. Photonics Healthcare B.V. holds the exclusive licenses to several patents regarding this technology, filed and owned by the Academic Medical Center in Amsterdam and the Erasmus Medical Center in Rotterdam, The Netherlands.

Sander I. A. Bodmer is a medical doctor and Ph.D. student at the Department of Anesthesiology at the Erasmus M.C. – University Medical Center Rotterdam, The Netherlands. His research focuses on the development and application of techniques for measuring microvascular oxygen tension based on in vivo use of phosphorescent nano-carriers.

Gianmarco M. Balestra is an internist and intensive care medicine specialist working as a consultant in the medical intensive care unit at the University Hospital Basel, Switzerland. His scientific interest includes the pathophysiological states of the microcirculation during critical illness and in particular the myocardial oxygenation states during sepsis. He conducts his research in close collaboration with the Laboratory of Experimental Anesthesiology of the Erasmus M.C. in Rotterdam.

Floor A. Harms is a medical doctor and Ph.D. student at the Department of Anesthesiology at the Erasmus M.C. – University Medical Center, Rotterdam. Her work focuses on mitochondrial oxygenation in sepsis, based on measurement of the oxygen-dependent delayed fluorescence of endogenous protoporphyrin IX.

Tanja Johannes is anesthesiologist and staff member at the Department of Anesthesiology at the Erasmus M.C. – University Medical Center Rotterdam, The Netherlands. She received her Ph.D. degree in 2011 from the University of Amsterdam. Her scientific interests include pathophysiological changes in kidney oxygenation in sepsis, studied with phosphorescence and delayed fluorescence lifetime techniques.

Nicolaas J. H. Raat is physiologist and researcher at the Department of Anesthesiology at the Erasmus M.C. – University Medical Center Rotterdam. He worked on the dietary effects of nitrite on ischemia reperfusion injury at the National Heart, Lung and Blood Institute at the NIH, Bethesda, M.D., USA and on the interaction

of nitrite and NO with hemoglobin at the Vascular Medicine Institute in Pittsburgh, PA, USA. His scientific interests include the effects of NO scavenging by stored blood and hemoglobin based oxygen carriers on oxygen metabolism.

Robert Jan Stolker is professor of anesthesiology and chairman of the Department of Anesthesiology at the Erasmus M.C. – University Medical Center Rotterdam, The Netherlands. Besides his interests in experimental anesthesiology his scientific work covers the fields of pain medicine and resident training.

Egbert G. Mik is anesthesiologist-intensivist and staff member at the Departments of Anesthesiology and Intensive Care at the Erasmus M.C. – University Medical Center Rotterdam, The Netherlands. He received his Ph.D. degree in 2011 cum laude from the University of Amsterdam. He is heading the Laboratory of Experimental Anesthesiology and his research focuses on tissue oxygenation and oxygen metabolism in the perioperative and intensive care setting.

References

[1] R. Springett and H. M. Swartz, Antioxid. Redox Signal. **9**, 1295–1301 (2007).
[2] D. W. Lubbers and H. Baumgartl, Kidney Int. **51**, 372–380 (1997).
[3] M. Sinaasappel, C. Donkersloot, J. van Bommel, and C. Ince, Am. J. Physiol. **276**, G1515–1520 (1999).
[4] H. M. Swartz and R. B. Clarkson, Phys. Med. Biol. **43**, 1957–1975 (1998).
[5] H. M. Swartz and J. Dunn, Adv. Exp. Med. Biol. **566**, 295–301 (2005).
[6] J. M. Vanderkooi, G. Maniara, T. J. Green, and D. F. Wilson, J. Biol. Chem. **262**, 5476–5482 (1987).
[7] V. Rozhkov, D. Wilson, and S. Vinogradov, Macromolecules **35**, 1991–1993 (2002).
[8] S. A. Vinogradov, L. W. Lo, and D. F. Wilson, Chem. Eur. J. **5**, 1338–1347 (1999).
[9] I. Dunphy, S. A. Vinogradov, and D. F. Wilson, Anal. Biochem. **310**, 191–198 (2002).
[10] D. C. Poole, B. J. Behnke, P. McDonough, R. M. McAllister, and D. F. Wilson, Microcirculation **11**, 317–326 (2004).
[11] T. Johannes, E. G. Mik, and C. Ince, J. Appl. Physiol. **100**, 1301–1310 (2006).
[12] S. A. Vinogradov, M. A. Fernandez-Seara, B. W. Dupan, and D. F. Wilson, Comp. Biochem. Physiol. A Mol. Integr. Physiol. **132**, 147–152 (2002).
[13] L. S. Ziemer, W. M. Lee, S. A. Vinogradov, C. Sehgal, and D. F. Wilson, J. Appl. Physiol. **98**, 1503–1510 (2005).
[14] T. Johannes, C. Ince, K. Klingel, K. E. Unertl, and E.G. Mik, Crit. Care Med. **37**, 1423–1432 (2009).
[15] T. Johannes, E. G. Mik, B. Nohe, N. J. Raat, K. E. Unertl, and C. Ince, Crit. Care **10**, R88 (2006).
[16] E. G. Mik, J. Stap, M. Sinaasappel, J. F. Beek, J. A. Aten, T. G. van Leeuwen, and C. Ince, Nat. Methods **3**, 939–945 (2006).
[17] F. A. Harms, W. M. de Boon, G. M. Balestra, S. I. Bodmer, T. Johannes, R. J. Stolker, and E. G. Mik, J. Biophotonics **5**, 731–739 (2011).
[18] E. G. Mik, C. Ince, O. Eerbeek, A. Heinen, J. Stap, B. Hooibrink, C. A. Schumacher, G. M. Balestra, T. Johannes, J. F. Beek, A. F. Nieuwenhuis, P. van Horssen, J. A. Spaan, and C. J. Zuurbier, J. Mol. Cell Cardiol. **46**, 943–951 (2009).
[19] E. G. Mik, T. Johannes, C. J. Zuurbier, A. Heinen, J. H. Houben-Weerts, G. M. Balestra, J. Stap, J. F. Beek, and C. Ince, Biophys. J. **95**, 3977–3990 (2008).
[20] A. S. Golub, A. S. Popel, L. Zheng, and R. N. Pittman, Biophys. J. **73**, 452–465 (1997).
[21] T. Johannes, E. G. Mik, and C. Ince, Shock **31**, 97–103 (2009).
[22] E. G. Mik, T. Johannes, and C. Ince, Am. J. Physiol. Renal Physiol. **294**, F676–681 (2008).
[23] R. Poulson, J. Biol. Chem. **251**, 3730–3733 (1976).
[24] H. Fukuda, A. Casas, and A. Batlle, Int. J. Biochem. Cell Biol. **37**, 272–276 (2005).
[25] J. van den Boogert, R. van Hillegersberg, F. W. de Rooij, R. W. de Bruin, A. Edixhoven-Bosdijk, A. B. Houtsmuller, P. D. Siersema, J. H. Wilson, and H. W. Tilanus, J. Photochem. Photobiol. B **44**, 29–38 (1998).
[26] R. N. Pittman, Acta Physiol. (Oxf) **202**, 311–322 (2011).
[27] D. F. Wilson, O. S. Finikova, A. Y. Lebedev, S. Apreleva, A. Pastuszko, W. M. Lee, and S. A. Vinogradov, Adv. Exp. Med. Biol. **701**, 53–59 (2011).
[28] D. F. Wilson, W. M. Lee, S. Makonnen, O. Finikova, S. Apreleva, and S. A. Vinogradov, J. Appl. Physiol. **101**, 1648–1656 (2006).
[29] P. A. Mole, Y. Chung, T. K. Tran, N. Sailasuta, R. Hurd, and T. Jue, Am. J. Physiol. **277**, R173–180 (1999).
[30] B. A. van Wagensveld, T. M. van Gulik, E. E. Gabeler, A. J. van der Kleij, H. Obertop, and D. J. Gouma, Eur. Surg. Res. **30**, 13–25 (1998).
[31] D. F. Wilson, Am J Physiol Heart Circ. Physiol. **294**, H11–13 (2008).
[32] S. Liu, S. J. Shah, L. J. Wilmes, J. Feiner, V. D. Kodibagkar, M. F. Wendland, R. P. Mason, N. Hylton, H. W. Hopf, and M. D. Rollins, Magn. Reson. Med. (2011).